

Copper Oxide Superconducting/Antiferromagnetic Interface

Yulii Kisilinskii^{1,4,a*}, Karen Constantinian^{1,b}, Gennady Ovsyannikov^{1,2,c},
Anton Shadrin^{1,e}, Igor Borisenko^{1,d}, Yuri Khaydukov^{3,f},
Alexander Sheyerman^{1,g}, Aleksandr Vasiliev^{5,h}

¹Kotel'nikov IRE RAS, 125009 Moscow, Russia

²Chalmers University of Technology, SE-41 296 Gothenburg, Sweden

³Max-Planck Institute for Solid State Research, 70 569 Stuttgart, Germany

⁴Shubnikov Institute of Crystallography, 119333 Moscow, Russia

⁵Kurchatov National Research Center, Moscow, Russia

^{a*}yulii@hitech.cplire.ru, ^bkaren@hitech.cplire.ru, ^cgena@hitech.cplire.ru,

^eanton_sh@hitech.cplire.ru, ^diboris@hitech.cplire.ru, ^fyury.khaydukov@frm2.tum.de,

^gsasha@hitech.cplire.ru, ^ha.vasiliev56@gmail.com

Keywords: accumulation and depletion of holes, band diagram, capacitance, high T_C Josephson junction, mesa-heterostructures, proximity effect, superconducting/antiferromagnetic interfaces.

Abstract. Superconducting Nb/Au/Ca_{1-x}Sr_xCuO₂/YBa₂Cu₃O₇ mesa-heterostructures were investigated. Dependencies of electrical parameters versus inverse capacitance were measured. A band diagram which takes into account an accumulation of holes in Ca_{1-x}Sr_xCuO₂ interlayer and band bending due to difference of work functions was proposed. The dependencies of electrical parameters were analyzed by examining the quasiparticle and superconducting currents.

Introduction.

Processes in interfaces are important for carrier transport in high critical temperature (T_C) Josephson junctions. In YBa₂Cu₃O₇/PrBa₂Cu₃O₇/YBa₂Cu₃O₇ (YBCO/PBCO/YBCO) junctions an accumulation of mobile holes into the p-type PBCO takes place, which results in conversion of hopping conductor PBCO into a metal up to 50 nm in depth [1]. In YBCO/La_{0.7}Sr_{0.3}MnO₃/YBCO junctions the manganite barrier provides depletion of the holes in p-type YBCO electrode and dielectric layer was formed [2]. Procedure to calculate hopping conductivity parameters from electrophysical properties of junctions was developed [3, 4]. Such high – T_C junctions usually exhibit I-V curves SNS – type [1, 5] and products of normal resistance R_N by critical current I_C are not very high. But up to now models of carrier transport and band diagrams for high – T_C junctions are qualitative [1,2] and require in-depth investigation.

Experimental.

We have fabricated Nb/Au/Ca_{1-x}Sr_xCuO₂/YBa₂Cu₃O₇ mesa-structures. Most of the data in this paper concern mesa-heterostructures with an interlayer made from G-type antiferromagnetic Ca_{0.5}Sr_{0.5}CuO₂ (AMS). Ca_{0.5}Sr_{0.5}CuO₂ (CSCO) could be treated as hopping conductor with resistivity at 300 K $\rho(300) \sim 10 - 100 \text{ m}\Omega \cdot \text{cm}$, which is more than for PBCO $\rho(300) \sim 1 \text{ m}\Omega \cdot \text{cm}$ [1]. The YBCO films of 100 nm thick were deposited on NdGaO₃ substrate by laser ablation. Without vacuum breaking CSCO layer was deposited at the same run. An epitaxial growth of YBCO and CSCO films was provided. A thin protection layer of 15 nm Au was deposited *in-situ*. Top layers of 200 nm Nb and Au contacts were made in other chamber. A square junctions with areas A from 10×10 to $50 \times 50 \mu\text{m}^2$ and with CSCO interlayer with thickness $d_M = 5 - 80 \text{ nm}$ were made [6].

Model and uniformity of mesa-heterostructures.

Superconducting current was observed for AMS with CSCO thickness $d_M=12 - 50$ nm with critical current density $J_C=I_C/A$ of $2 - 600$ A/cm². Magnetic field dependencies $I_C(H)$ were studied. Fig. 1 demonstrates dependence of I_C vs. magnetic field at 4.2 K for AMS with relatively thin $d_M=20$ nm, $A=10 \times 10$ μm². The up triangles are positive current biased critical currents and down triangles – negative ones. Singularities on $I_C(H)$ are caused by antiferromagnetic (AF) interlayer and are less pronounced than in [7] due to large $J_C=350$ A/cm². The main I_C oscillation period is of $B_0 \approx 45$ μT. It has double width at $H=0$ that points on uniformity of critical current distribution at least for AMS with $d_M \geq 20$ nm. Field period B_0 estimated by differences between $I_C(H)$ minima in Fig. 1 gives an effective area for magnetic field penetration of 5 μm². The period was of 10 times smaller than the B_0 periods for mesa-structures without CSCO interlayer (MS). Small B_0 of AMS compared to B_0 of MS were observed earlier for other CSCO thicknesses [7]. This was explained by giant magnetic oscillations of critical currents of S-AF-S junctions [8].

A band diagram of the AMS is presented in Fig. 2. A YBCO electrode has high work function Φ_{YBCO} 5 – 6 eV [2]. The work functions of metals are low $\Phi_{Au}=4.3$ eV, $\Phi_{Nb}=4$ eV. We suppose that electron affinity of CSCO χ_{CSCO} is between: $\Phi_{YBCO} > \chi_{CSCO} > \Phi_{Nb}$. So, free holes from YBCO accumulate in p-type CSCO [1]. It is shown by up band bending in Fig. 2. By reference [2] if condition $\chi_{CSCO} > \Phi_{Nb}$ is fulfilled a depletion of holes appears in CSCO at Au interface, band bending is down. Total bending in AMS is equal to difference in work functions $\Phi_{YBCO}-\Phi_{Nb}=1-2$ eV.

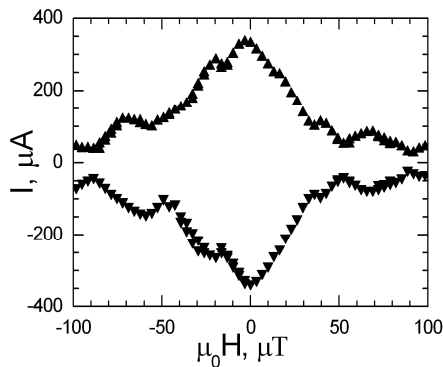


Fig. 1. I_C versus magnetic field dependence at 4.2 K for AMS with $d_M=20$ nm, $A=10 \times 10$ μm². Up triangles are positive biased critical currents and down triangles – negative ones.

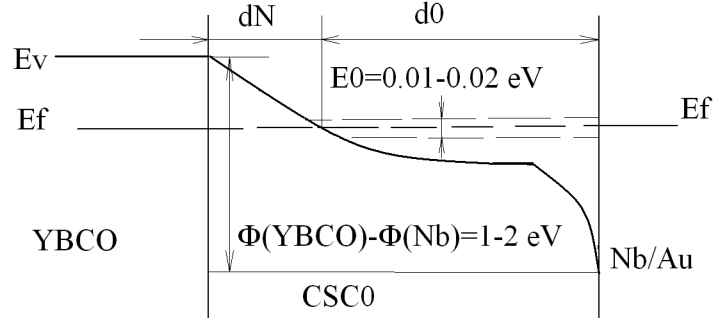


Fig. 2. Band diagram of AMS with CSCO barrier layer. Valence band E_V in YBCO and CSCO is shown as the bold line. Fermi level (dash line) is a constant in whole structure. Hopping sub-band of CSCO with an average barrier height E_0 is thin dash lines. Difference in work functions Φ is shown.

A hopping conductor has conductivity dependency $G(T)=G_0 \exp[-(T_0/T)^{1/4}]$ that exponentially decreases with lowering the temperature. Experimental constant T_0 depends on carrier localization radius a and density of states at Fermi level g as $T_0=24/(\pi k g a^3)$, k is Boltzmann constant. Details of the calculations for junctions with hopping conductor were described in [3]. By localization radius CSCO $a=5 \pm 2$ nm and by $T_0 \sim 10^6$ K we have calculated $g=(0.2 - 5) \cdot 10^{18}$ (eV)⁻¹cm⁻³ in [6].

Conductivity by resonant tunneling with average barrier height E_0 is $G_{res}=(\pi e^2/\hbar)E_0 \cdot g a \cdot \exp(-d/a)$. For dielectric thickness $d \rightarrow 0$ it is $G_{res}=(\pi e^2/\hbar)E_0 \cdot g a$. By measured G/A versus d dependency and known values g and a barrier height in YBCO/PBCO/Au junctions was calculated $E_0=51$ meV [3]. We calculate the average height as $E_0=(h/2\pi^2 e^2)/[g a \cdot R_{NA}(d \rightarrow 0)]$. The $R_{NA}(d \rightarrow 0) \approx 0.18$ μΩcm² was extrapolated from experimental dependency of resistance on area products versus CSCO thickness: $R_{NA}(d_M)$ [6]. The calculated value for CSCO is $E_0=10 - 20$ meV. The band diagram shows that there are metallic - type layer with thickness d_N and dielectric-type layer with thickness d_0 .

Dependencies of electrical parameters and interface capacitance.

A dielectric thickness d_0 may be less than interlayer thickness d_M if the accumulation takes place [1]. Dependence d_0 versus d_M was calculated from C - capacitance of AMS [6]. By hysteresis of voltage-current curves McCumber parameters were calculated by Zappe formula [9]:

$\beta_C = [2 - (\pi - 2)\alpha] \alpha^{-2}$, $\alpha = I_{RETURN}/I_C$. By McCumber definition $\beta_C = 4\pi e I_C R_N^2 C/h$ and for $C = \epsilon \epsilon_0 A/d_0$:

$$\frac{d_0}{\epsilon} = \epsilon_0 \frac{A}{C} = \frac{4\pi \epsilon_0}{h} \cdot \frac{A I_C R_N^2}{\beta_C} \quad (1)$$

We have calculated dielectric thickness d_0 from experimental A/C values. Calculation by (1) shows increase of d_0/ϵ from $d_0/\epsilon = 0.24 \pm 0.08$ at $d_M = 12$ nm to $d_0/\epsilon = 11.7 \pm 2.9$ nm at $d_M = 50$ nm. Layer which does not contribute to capacitance could be extracted by the d_0/ϵ dependency vs. d_M [6]. This layer with a thickness of $d_N \approx 20$ nm has metallic type behavior. For samples with $d_M > 20$ nm there is a wide dielectric layer $d_0 \approx d_M - d_N$. Dependence of $R_N A$ versus d_0/ϵ ratios is shown in Fig. 3.

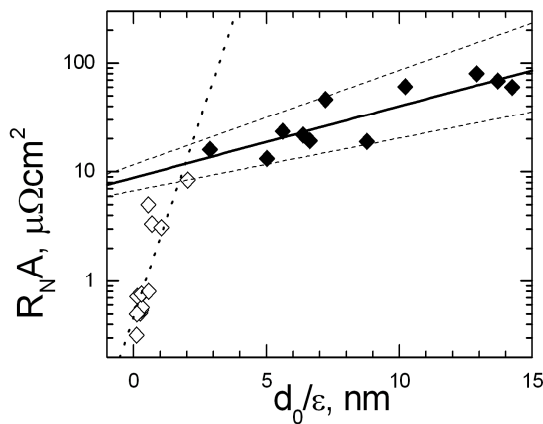


Fig. 3. Dependency of $R_N A$ of AMS versus d_0/ϵ . Open symbols are data for AMS with $d_M \leq 20$ nm, exponential approximation for the data is dotted line. Closed symbols show data for samples with $d_M > 20$ nm, exponential approximation – solid line, it's standard deviation – dashed lines.

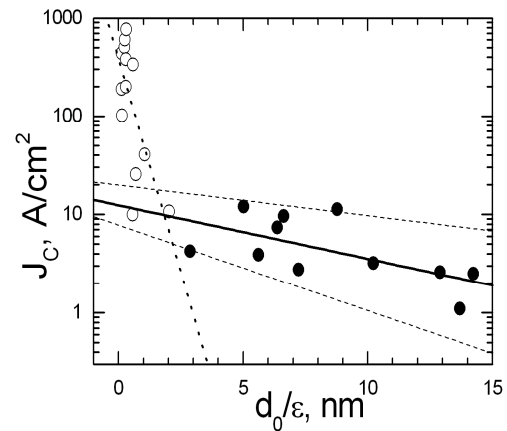


Fig. 4. Dependency of current densities versus d_0/ϵ . Open symbols are data for AMS with $d_M \leq 20$ nm, exponential fit is dotted line. Closed symbols – data for $d_M > 20$ nm, it's exponential approximation – solid line, standard deviation shown as dashed lines.

In Fig 3 data for AMS with small CSCO thicknesses $d_M = 12, 20$ nm and for thicker CSCO with $d_M = 28, 40, 50$ nm were fitted separately by steep and smooth sloping exponents. The fits are:

$$R_N A = k_{RS} \exp\left(\frac{d_0/\epsilon}{a_{RS}}\right) \quad d_M \leq 20 \text{ nm}, \quad R_N A = k_{RG} \exp\left(\frac{d_0/\epsilon}{a_{RG}}\right) \quad d_M > 20 \text{ nm}. \quad (2)$$

For steep exponent by a least squares fit method we obtain coefficients $k_{RS} = 0.5 \mu\Omega \text{cm}^2$, $a_{RS} = 0.6$ nm that is shown by dotted line in Fig 3. For AMS with $d_M > 20$ nm the exponential increase was more smooth: $k_{RG} = 9 \mu\Omega \text{cm}^2$, $a_{RG} = 6.6$ nm that is solid line. An error of calculation of the coefficient gives interval $5 < a_{RG} < 9$ nm that is shown as dashed lines.

Dependency of critical current density J_C versus ratio of d_0/ϵ is shown in Fig 4. The fits are:

$$J_C = k_{JS} \exp\left(-\frac{d_0/\epsilon}{a_{JS}}\right) \quad d_M \leq 20 \text{ nm}, \quad J_C = k_{JG} \exp\left(-\frac{d_0/\epsilon}{a_{JG}}\right) \quad d_M > 20 \text{ nm}. \quad (3)$$

A steep exponential decrease with coefficients $k_{JS} = 380 \text{ A/cm}^2$, $a_{JS} = 0.5$ nm was obtained by the least squares fit. Dependence for AMS with $d_M > 20$ nm gives the parameters: $k_{JG} = 12.5 \text{ A/cm}^2$, $a_{JG} = 8.0$ nm. It is shown as solid line in Fig. 4. The error interval $5 < a_{JG} < 14$ nm is shown as dashed lines.

From Fig. 3 and Fig. 4 we conclude that transport mechanism in AMS changes during increase of thickness approximately at $d_M=20$ nm. In case of $d_M \leq 20$ nm the steep slopes in $R_{NA}(d_0/\epsilon)$ and $J_C(d_0/\epsilon)$ dependencies may be explained by direct tunneling through thin barrier at CSCO/Au interface (Fig. 2). The barrier thickness may be estimated by $\epsilon \sim 2$ and $d_0/\epsilon = 0.24 - 1$ nm (Fig. 3) that gives $d_0 \sim 0.5 - 2$ nm. The rest of CSCO layer is metallic – type due to the accumulation. The height of a rectangular barrier may be estimated as: $E_b \sim \hbar^2 / (8\pi m_e a_D^2)$ with $m_e = 9 \cdot 10^{-31}$ kg. Characteristic length a_D may be obtained by dependencies for direct tunneling: $J_C \sim \exp(-2d/a_D)$, $R_{NA} \sim \exp(2d/a_D)$. Compared the dependencies with formula (2) and (3) one obtains $a_D \sim 2\epsilon \cdot a_{RS}$, $a_D \sim 2\epsilon \cdot a_{JS}$ that gives $a_D \sim 4a_{JS} = 2$ nm and $E_b \sim 10$ meV. The coefficients are the same $a_{RS} \sim a_{JS}$, thus $I_C R_N(d_0) \sim \text{const}$.

Because $a_{RG} \sim a_{JG}$ one obtains $V_C(d_0) \sim \text{const}$ for $d_M > 20$ nm also. Large values of $a_{RG} \sim 10a_{RS}$ and $a_{JG} \sim 10a_{JS}$ lead to a barrier height $E_b \sim a_D^{-2} \approx 0.1$ meV small compared to $kT \approx 0.36$ meV at 4 K. So direct tunneling can not explain the smooth exponential slopes. Other explanation may be proximity effect which originates from resonant tunneling through pair states in CSCO barrier [10]. In case of narrow widths of energy states $\Gamma = E_0 \exp(-d_0/a) < kT_C$ the pair breaking occurs. In opposite limit $\Gamma > kT_C$ if Cooper pairs tunnel via resonant levels [10], it also yields $V_C(d_0) = \text{const}$.

Note, at localization radius $a \approx 1$ nm no supercurrent was observed through PBCO interlayer 7.5 nm in thickness [3], but for larger $a \approx 3$ nm and PBCO thickness 20 nm a Josephson current was reported in [4]. In our AMS with superconducting/antiferromagnetic interfaces large radii a in $\text{Ca}_{0.5}\text{Sr}_{0.5}\text{CuO}_2$ antiferromagnetic interlayer support long proximity effect and result in experimentally observed decrease of quasiparticle current with d_M , keeping V_C very slightly dependent from CSCO thickness.

Acknowledgment

This work was supported partially by the RAS, RFBR projects 14-07-00258, 14-07-93105, Scientific School grant NSH-4871.2014.2. P.V. Komissinski is grateful for fruitful discussions.

References

- [1] M.I. Faley, U. Poppe, C.L. Jia, K. Urban, Order and interface effects in $\text{YBa}_2\text{Cu}_3\text{O}_7$ - $\text{PrBa}_2\text{Cu}_3\text{O}_7$ - $\text{YBa}_2\text{Cu}_3\text{O}_7$ Josephson junctions, IEEE Trans. on Appl. Super. 7 (1997) 2514 – 2517.
- [2] M. Van Zalk, A. Brinkman, J. Aarts, H. Hilgenkamp, Interface resistance of $\text{YBa}_2\text{Cu}_3\text{O}_7$ / $\text{La}_{0.7}\text{Sr}_{0.3}\text{MnO}_3$ ramp-type contacts, Physical Rev. B 82 (2010) 134513-1 – 134513-9.
- [3] J. Yoshida, T. Nagano, Tunneling and hopping conduction via localized states in thin $\text{PrBa}_2\text{Cu}_3\text{O}_7$ barriers, Physical Rev. B 55 (1997) 11860 – 11871.
- [4] J. Yoshida, T. Nagano, T. Hashimoto, Current transport and electronic states in a, b- axis-oriented $\text{YBa}_2\text{Cu}_3\text{O}_7$ / $\text{PrBa}_2\text{Cu}_3\text{O}_7$ / $\text{YBa}_2\text{Cu}_3\text{O}_7$ sandwich type junctions, Physical Rev. B 53 (1996) 8623 – 8631.
- [5] S. Charpentier, G. Roberge, S. Godin-Proulx, P. Fournier, Proximity effect in electron-doped cuprate Josephson junctions, Applied Phys. Lett. 99 (2011) 032511-1 – 032511-3.
- [6] K.Y. Constantinian, Yu.V. Kislinskii, G.A. Ovsyannikov, A.V. Shadrin, A.E. Sheyerman, A.L. Vasiliev, M.Yu. Presnyakov, P.V. Komissinskiy, Interfaces in superconducting hybrid heterostructures with an Antiferromagnetic Interlayer, Physics of the Solid State. 55, (2013) 461 – 465.
- [7] Yu.V. Kislinskii, K.Y. Konstantinian, G.A. Ovsyannikov, P.V. Komissinskiy, I.V. Borisenko, A.V. Shadrin, Magnetically dependent superconducting transport in oxide heterostructures with an antiferromagnetic layer, JETP 106 (2008) 800 – 805.
- [8] L.P. Gorkov, V.Z. Kresin, Mixed-valence manganites: fundamental and main properties, Physics reports 400 (2004) 149 – 208.
- [9] H.H. Zappe, Minimum current and related topics in Josephson tunnel junction devices, Journal of Appl. Phys. 44 (1973) 1371 – 1377.
- [10] I. A. Devyatov, M.Yu. Kupriyanov, Resonant tunneling and long-range proximity effect, JETP Letters, 59 (1994) 200 – 205.